WWJMRD 2021; 7(1): 25-36
www.wwjmrd.com
International Journal
Peer Reviewed Journal
Refereed Journal
Indexed Journal
Impact Factor MJIF: 4.25
E-ISSN: 2454-6615

Alfred Rufer
EPFL, Ecole Polytechnique
Fédérale de Lausanne
Lausanne, CH1015,
Switzerland.

Correspondence:
Alfred Rufer
EPFL, Ecole Polytechnique
Fédérale de Lausanne
Lausanne, CH1015,
Switzerland.
alfred.rufer@epfl.ch

A High Efficiency Pneumatic Motor Based on Double-Acting Linear Cylinders

Alfred Rufer

Abstract
A high efficiency pneumatic motor is presented, based on the coupling of two double-acting linear cylinders. The pneumatic motor is used in a chain of compressed air energy storage and drives an electric generator. The principle of coupling two cylinders of different sections allows to produce, in addition to the normal displacement work of the cylinders an additional amount of expansion work. This additional work finally elevates the total conversion efficiency of the motor, in comparison with the efficiency of a motor using a simple cylinder without expansion work and consuming an identical quantity of compressed air from the feeding reservoir. The use of cylinders with a section ratio of four leads to a doubling of the energy efficiency. The paper includes the simulation of a single cylinder system as well as the new proposed motor. Pressures in the chambers are presented as well as the developed torques at the output of the crankshaft. The paper includes the calculation of the efficiencies, based on the injected enthalpy. Then, the paper presents an original evolution of the motor in which the same performance can be achieved with one cylinder only. Finally, the paper presents an experimental set-up realized at a low power level.

Keywords: Compressed air motor; energy efficiency; adiabatic expansion; compressed air energy storage; pneumatic cylinder

Introduction
In the context of the development of renewable energy sources the question of energy storage often appears as an important challenge. Beneath the classical solutions based on electrochemical batteries, alternative solutions as compressed air energy storage (CAES) have been proposed with the argument of being better suited for longer life cycles and free from recycling problems of the used materials [1], [2], [3]. For a significant energy density of a CAES system, high pressure of the storage vessel is demanded, together with compression and expansion processes in near isothermal conditions [4], [5], [6]. Such complex equipment leads to high design costs and important invested grey energy.
Especially regarding the ratio of the needed investment for the realization to the amount of storable energy during the life cycle of the equipment, an original solution consists in storing the compressed air in immersed flexible underwater bags, the so called UWCAES. [7]. [8], [9]. For those installations, a limited depth of immersion means a limited storage pressure but has the advantage of being operated in the full storage capacity under constant pressure conditions [3]. Another condition for viable CAES systems is the energetic efficiency of the compression and expansion machines. This is the main concern of this paper, describing a pneumatic motor driving an electric generator as one element of the complete storage chain. Such a motor can be realized on the base of linear piston/cylinder devices available as high-volume industrial components. In such a system, the linear movement of the piston is converted into the rotational motion using a conventional crankshaft and connecting rod.
In order to increase the energetic efficiency, a pneumatic motor concept using two linear cylinders of different sections is described. In this concept, the linear cylinder pistons are connected to a classical crankshaft with crankshaft-pins shifted of 180°. This concept is based on the combination of an elementary work production with displacement of the piston under constant pressure with an additional work of thermodynamic expansion, leading to an augmented energetic efficiency [10], Fig. 1.

First, the dynamics of the piston/crankshaft assembly are given, with relations to calculate the torque and the produced mechanical work.

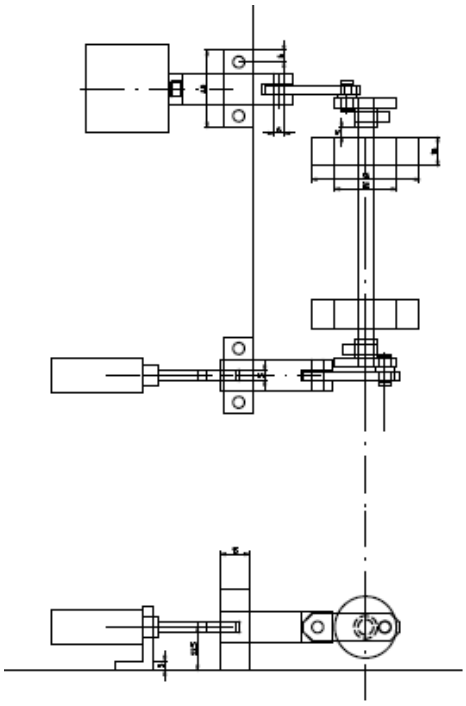

Fig. 1: Pneumatic motor with enhanced efficiency.

Then a simple pneumatic motor is described as a reference, where the cylinder works according the classical principles of pneumatic devices, namely with only a succession of sequences with constant pressure displacement work. The typical variables are simulated as the dynamics of the piston/crankshaft assembly and the developed torque. The energetic performance of this elementary motor is then evaluated.

After that, a pneumatic motor with enhanced efficiency is described where an additional expansion chamber is coupled to the first single piston system. Pressures, forces and torques are simulated. Finally, the energetic performance is calculated and compared to the performance of the single cylinder system. An experimental system is also realized.

In the last section of the paper, an original motor is presented in which the same performance can be achieved with a one-cylinder motor in which the displacement work and the expansion are realized in the same chamber with the help of a dedicated valve control system.

The Elementary System

Mathematical description of the piston/crankshaft assembly

In Fig.2 the piston is represented with the connecting rod and the crankshaft. The parameters are indicated as r, the radius of the crankshaft, l the length of the connecting rod, and Φ the angle of rotation of the crankshaft. The diameter of the piston, d and its position x are also indicated.

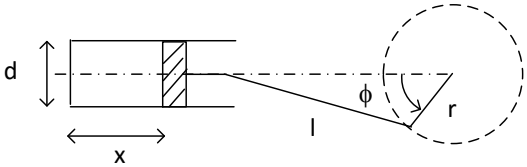

Fig. 2: Piston, crankshaft and connecting rod.

The position of the piston is given through rel. (1)

$$x = r(1 - cos\,\varphi) + \frac{\lambda}{2} r\, sin^2\,\varphi \quad (1)$$

where the connecting rod ratio l is used and is defined as

$$\lambda = \frac{r}{l} \quad (2)$$

The velocity of the piston is given by

$$v = \omega \cdot r \cdot sin\,\varphi\,(1 + \lambda\, cos\,\varphi) \quad (3)$$

In the simulation process, the torque developed by the motor is calculated through the indirect calculation of the power. If the force exerted on the piston is given by

$$F_p = p \cdot A \quad (4)$$

the mechanical power is defined by the product of the force by the piston's velocity:

$$Pow = F_p \cdot v \quad (5)$$

The torque is obtained by the division of the power by the angular velocity w

$$M_{mot} = Pow/\omega \quad (6)$$

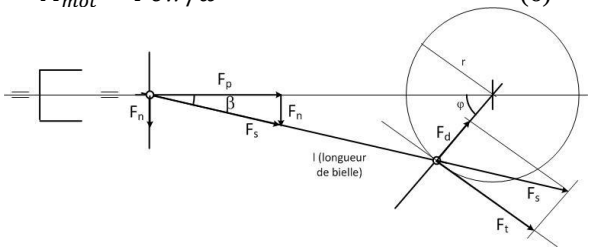

Fig. 3: Diagram of the forces for the calculation of the torque and reactions.

A direct calculation of the torque is however possible with the extended model represented in Fig. 3. The force on the connecting rod F_s, the tangential force F_t and the reaction force F_n are also defined. The torque on the crankshaft is given by rel.7.

$$M_{mot} = F_t \cdot r \quad (7)$$

The tangent force F_t is given by (8)

$$F_t = F_s\, cos(\pi/2 - (\beta + \varphi)) \quad (8)$$

The force transmitted through the connecting rod F_s is calculated with the help of the piston force F_p and the angle beta (9)

$$F_s = \frac{F_p}{cos\,\beta} \quad (9)$$

This angle is given by rel. (10)

$$\beta = arc\,sin\left(\frac{r}{l} \cdot sin\,\varphi\right) \quad (10)$$

The perpendicular reaction F_n is defined as per (11)

$$F_n = F_s\, sin\,\beta = \frac{F_p}{cos\,\beta} sin\,\beta \quad (11)$$

Simulation of a motor with one double acting cylinder

A pneumatic motor is simulated where one double acting cylinder is used. The dimensions of the cylinder are:

Diameter d=16mm

The stroke is given by twice the radius of the crankshaft, namely Xa = 2*r =20mm

The motor is running with a constant rotational speed, namely ω = 31.4 rad/s

First, the position of the piston is represented in Fig.4. The simulation lasts over two periods.

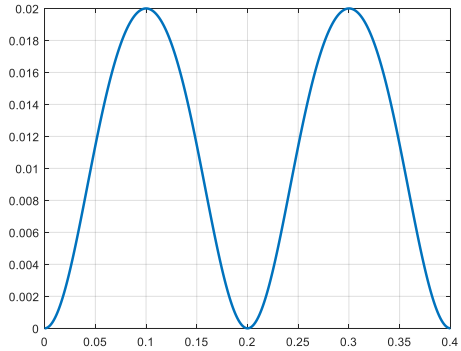

Fig. 4: Position of the piston.

Then, the velocity of the piston is shown on Fig. 5. The curve shows the typical form due to the specific connecting rod ratio.

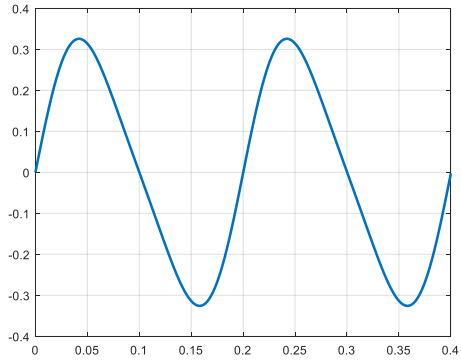

Fig. 5: Velocity of the piston.

The cylinder is fed with compressed air at a pressure of 10 bar. The air is brought alternatively to the left and to the right side of the piston. The control valves are activated at the top and bottom dead centres. These points correspond to angles of 0° and 180°.

The 16 mm diameter of the piston corresponds to a surface of

$$A = \frac{\pi d^2}{4} = 201 - mm^2 - or - 201 \cdot 10^{-6} m^2 \quad (12)$$

The force caused by the air pressure (first half period) is

$$F = A \cdot p = 201 \cdot 10^{-6} m^2 \cdot 10 \cdot 10^5 N/m^2 = 201N \quad (13)$$

On the opposite side of the piston, the atmospheric pressure causes a counter force of 20.1N, and the total force exerted on the piston becomes

$$F_{tot} = 201N - 20.1N = 180.9N \quad (14)$$

The total force is represented on Fig. 6

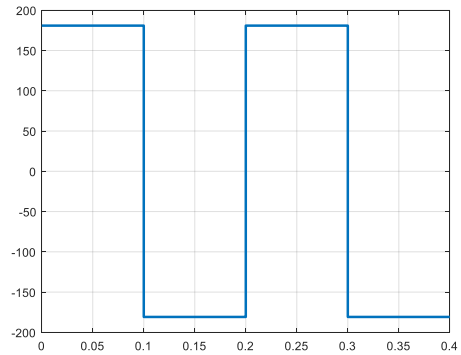

Fig. 6: Force on the 16 mm piston (no expansion).

The calculation of the torque applied to the crankshaft is done using the instantaneous value of the power. This quantity can be calculated through:

$$P = F_{tot} \cdot v \quad (15)$$

The evolution of the power is shown on Fig 7

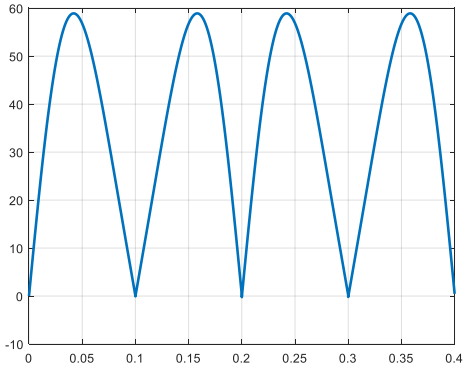

Fig. 7: Power developed by the 16 mm piston.

Then the torque follows as

$$M_{tot} = \frac{P}{\omega} \quad (16)$$

and is represented in Fig. 8

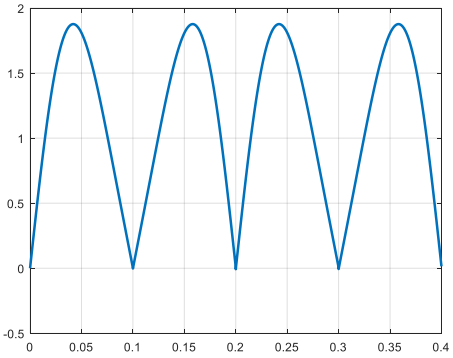

Fig. 8: Torque produced by the 16 mm piston (no expansion).

Energetic efficiency

The energetic efficiency of the motor is evaluated by calculation of the ratio of the mechanical energy obtained at the output to the enthalpy injected at the input of the pneumatic actuator.

The transmitted mechanical energy is obtained from the simulation curve of Fig. 9 It corresponds to the time integral of the instantaneous power according rel. 17. The final value of the converted energy is equal to 14.46 J

$$W_{out} = \int_0^t P(t)dt \quad (17)$$

$W_{out} = 14.46J$

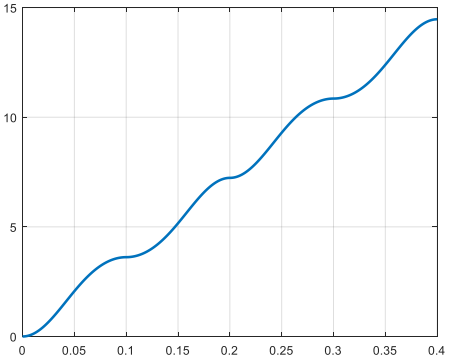

Fig. 9: Energy transmitted from the 16 mm piston.

The efficiency is calculated through rel. (18)

$$\eta_{conv} = \frac{W_{out}}{H_{in}} = \frac{W_{out}}{U + P_{in} \cdot \Delta V} \quad (18)$$

U is the thermodynamic content of the injected air under

pressure and is calculated as the energy needed for the compression into V_1 of the equivalent mass of air from the atmospheric pressure to the value of P_{in}, V_1 being the filled volume of the actuator during the total duration of the simulation (2 periods).

The fully expanded volume of one chamber of the 16 mm piston system is

$$V_{16\_max} = d^2 \frac{\pi}{4} \cdot 2r = (0.016)^2 \frac{\pi}{4} \cdot 0.02 = 4.02 \cdot 10^{-6} m^3 \quad (19)$$

$$V_{16\_max} = d^2 \frac{\pi}{4} \cdot 2r = (0.016)^2 \frac{\pi}{4} \cdot 0.02 = 4.02 \cdot 10^{-6} m^3 \quad (19)$$

and

$$U = E_{comp} = P_{in} \cdot V_1 \left(ln \frac{P_{in}}{P_{atm}} - 1 + \frac{P_{atm}}{P_{in}} \right) \quad (20)$$

Numerically, and considering the two complete cycles (ϕ =0…4π), U becomes

$$U = E_{comp} = 10 \cdot 10^5 N/m^2 \cdot 4 \cdot 4.02 \cdot 10^{-6} m^3 \cdot \left(ln \frac{10bar}{1bar} - 1 + \frac{1bar}{10bar} \right) = 22.5J \quad (21)$$

$$P_{in} \cdot \Delta V = 10 \cdot 10^5 N/m^2 \cdot 4 \cdot 4.02 \cdot 10^{-6} m^3 = 16J \quad (22)$$

The efficiency becomes

$$\eta_{conv} = \frac{W_{out}}{H_{in}} = \frac{14.46J}{16J + 22.55J} = 0.375 \quad (23)$$

The High Efficiency Motor

A pneumatic motor with enhanced efficiency - adding an expansion chamber

Fig. 10 shows the pneumatic motor with enhanced efficiency. In addition to the first cylinder, a second one is coupled to the crankshaft. The two cylinders are moving in phase opposition. They have different sizes but have the same stroke. They are working in a cascaded way, meaning that the compressed air is feeding the small cylinder during the first half period (first stroke), and is then transferred in the chamber of the second larger cylinder, producing the expected expansion and providing additional work to the output.

In the studied system, the cylinders have diameters of 16mm and 32mm. The stroke of both actuators is equal to 20mm.

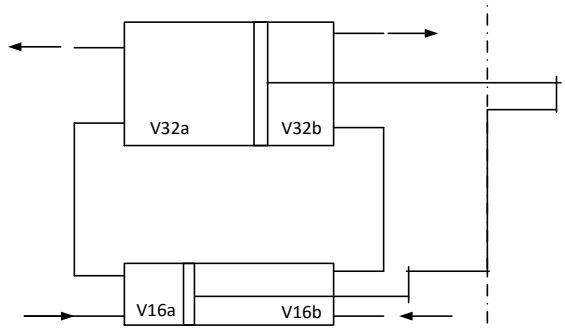

Fig. 10: Pneumatic motor with additional expansion chamber.

The factor two of the diameter of the cylinders imposes a ratio of four concerning the volumes.

The volume of the 16 mm cylinder is equal to

$$V_{16\_max} = d^2 \frac{\pi}{4} \cdot 2r = (0.016)^2 \frac{\pi}{4} \cdot 0.02 = 4.02 \cdot 10^{-6} m^3 \quad (24)$$

$$V_{16\_max} = d^2 \frac{\pi}{4} \cdot 2r = (0.016)^2 \frac{\pi}{4} \cdot 0.02 = 4.02 \cdot 10^{-6} m^3$$

and the volume of the 32 mm cylinder is

$$V_{32\_max} = d^2 \frac{\pi}{4} \cdot 2r = (0.032)^2 \frac{\pi}{4} \cdot 0.02 = 16.08 \cdot 10^{-6} m^3 \quad (25)$$

$$V_{32\_max} = d^2 \frac{\pi}{4} \cdot 2r = (0.032)^2 \frac{\pi}{4} \cdot 0.02 = 16.08 \cdot 10^{-6} m^3$$

The operating cycle is defined by the following steps:

1) Filling of the small volume (V16a for 0° to 180°, respectively V16b for 180° to 360°)
2) Transfer from the small volume (V16a for 180° to 360°, respectively 16b for 0° to 180°) into the larger one (V32a, respectively V32b).

The crankshaft with its crankpins placed at 0° and 180° defines the alternations between fillings and transfers. The control signals for the valves are generated from a position sensor.

The pressure in the cylinders is constant during the fillings and varies during the transfer from the small volumes to the larger ones. The pressure changes are defined according an adiabatic expansion curve given by rel 26

$$P_2 = P_1 \left(\frac{V_1}{V_2} \right)^{1.4} \quad (26)$$

The different volumes of the cascaded cylinders are indicated in the schematic representation of Fig. 10.

Simulation results

The behaviour of a pneumatic motor with two complementary cylinders is simulated. First, the position and velocity of the two pistons are simulated. The changes in the pressures in the respective cylinders is also calculated. Then, the torque contributions of the small and of the larger cylinders are represented.

Position and velocity of the two pistons

First the positions of the two alternating pistons are represented in Fig. 11, and their velocity in Fig. 12.

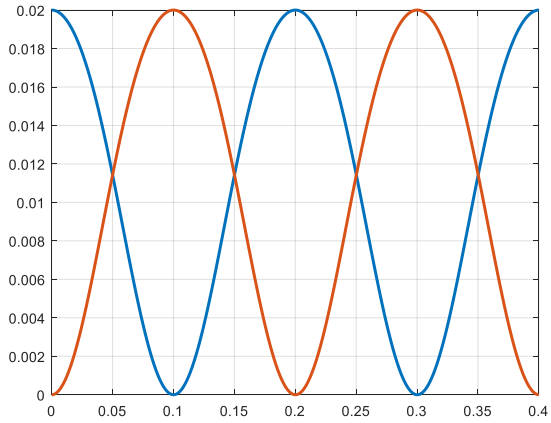

Fig. 11: Positions of the two cylinders.

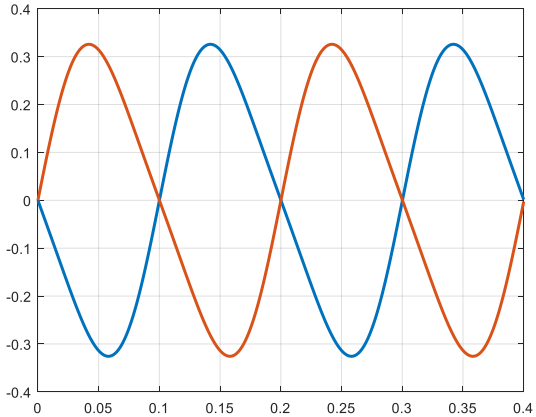

Fig. 12: Velocity of the two pistons.

Contributions of the 16 mm piston

The pressure level in the chambers of first cylinder are imposed from the air supply during the first half period (the filling). Then, the pressure is given by the expansion of the air into the second cylinder. The pressures in the alternating chambers of the 16 mm cylinder are represented in Fig. 13.

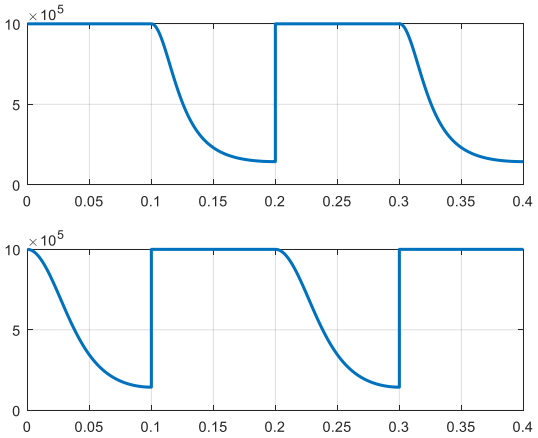

Fig. 13: Pressures in the chambers of the 16 mm cylinder

From the pressures in the volumes of the first cylinder, the corresponding force is calculated according.

$$F = A \cdot p \qquad (27)$$

The curves of the forces in the left volume (16a) and in the right volume (16b) are represented in Fig.14. These forces are represented according a convention of the normal axis to the surfaces of the piston. These forces are positive.

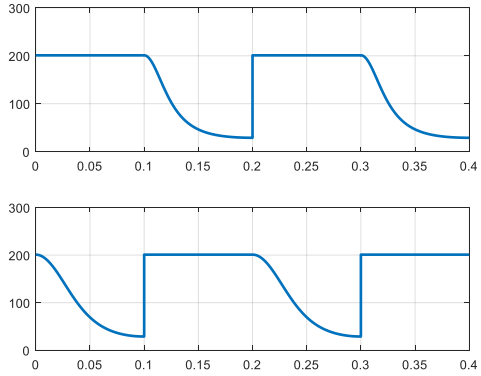

Fig. 14: Forces exerted on the two sides of the 16 mm piston.

The resulting force of the 16 mm cylinder is represented in Fig. 15 In this representation, the resulting force on the piston shows its direction. It is positive in the first half period (movement from left to the right), and negative in the other direction (180°-360°, movement from the right to the left).

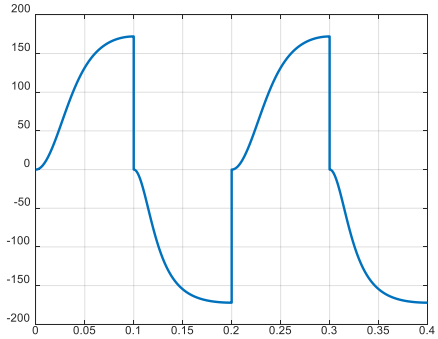

Fig. 15: Resulting force exerted by the 16 mm piston.

The resulting force is then multiplied by the piston's velocity to obtain the instant value or the mechanical power. This power concerns only the contribution of the 16mm piston.

$$P = v \cdot F \qquad (28)$$

The corresponding curve is shown in Fig. 16

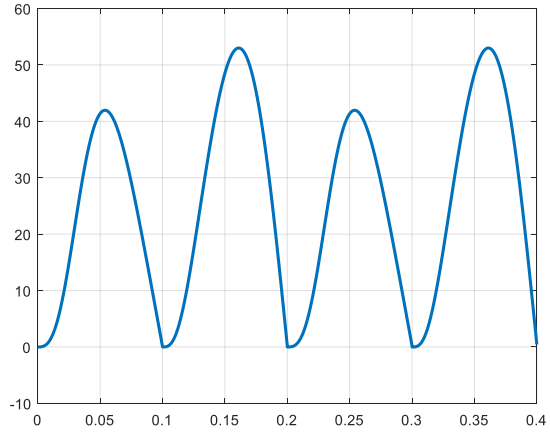

Fig. 16: Power developed by the 16 mm piston.

The developed mechanical power of the 16 mm piston on the crankshaft is then divided by the angular speed, leading to the profile of the torque.

$$M_{16} = P/\omega \qquad (29)$$

The corresponding curve is represented in Fig. 17

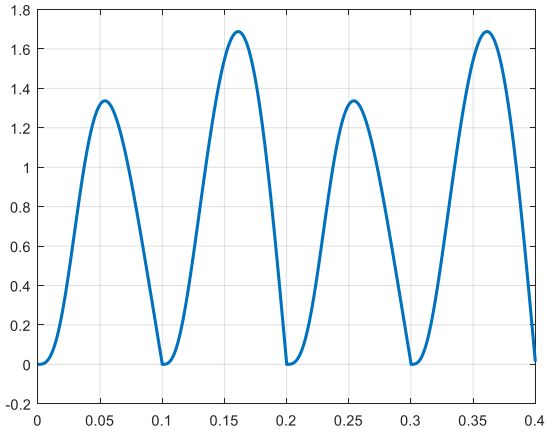

Fig. 17: Torque developed by the 16 mm piston.

Contributions of the second piston

Fig. 18 shows the evolution of the pressure in the volumes of the second cylinder (the 32mm cylinder). The first curve shows the pressure in the left side chamber V32a, where the pressure is equal to the atmospheric pressure during the

first half period (0°-180°). This phase of the sequence corresponds to the exhaust phase where the expanded mass of air is released to the atmosphere. During this phase the piston is moving from right to the left, while the 16mm piston moves from left to the right.
During the second half period (180°-360°), the pressure is decreasing from the level of the filling ($10*10^5$ N/m^2), down to the level of $1.43*10^5$ N/m^2. This corresponds to an adiabatic expansion with a volume ratio of ¼.

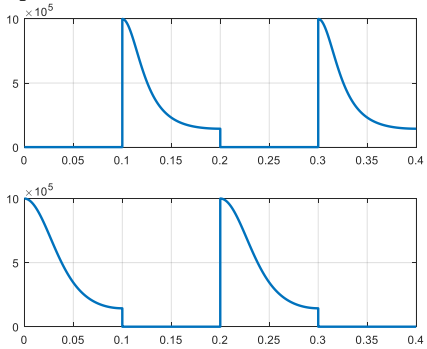

Fig. 18: Pressures in the chambers of the 32 mm cylinder.

The second curve shows the pressure in the right chamber of this cylinder (V32b). The phases of exhaust and of expansion alternate all 180°, but are in opposite angular position in reference to the left side chamber.
One can note the not identical evolutions of the expansions in the left and in the right chambers, this is due to the different evolution of the position of the piston in the first and second half periods. This is related to the not identical speed profile of the pistons with the specific ratio of the radius of the crankshaft to the length of the connecting rod.
In the next figure (Fig. 19), the forces on the left and right sides of the 32mm piston are represented. In these curves the influence of the atmospheric pressure during the exhaust phases is taken in account.

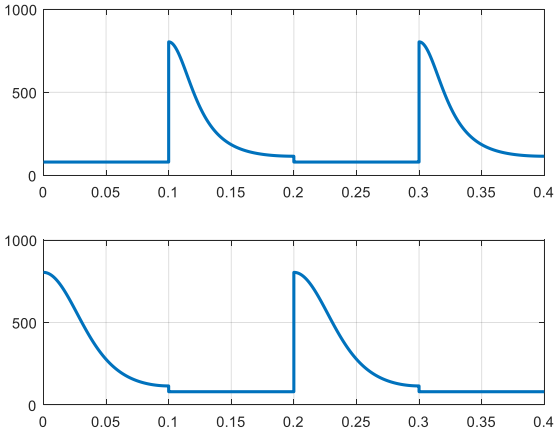

Fig. 19: Forces exerted on the 32 mm piston.

For the calculation of the torque contribution of this cylinder, the same method as for the first cylinder is used, namely a calculation through the piston's power. The power curve of the 32 mm piston is shown in Fig. 20.

$$P = v \cdot F \quad (30)$$

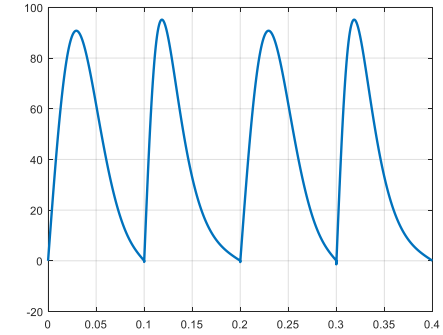

Fig. 20: Power curve of the 32 mm piston

From the power curve, the torque is calculated.

$$M_{32} = P/\omega \quad (31)$$

The evolution of the torque M_{32} is represented in Fig. 21.

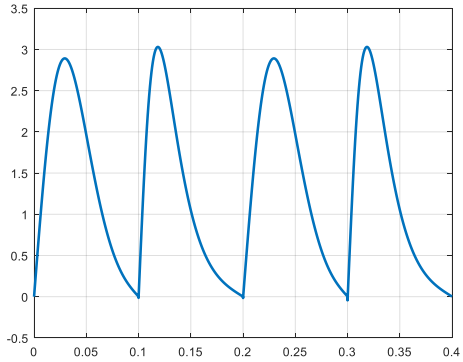

Fig. 21: Torque contribution of the 32 mm piston.

The total torque of the motor

The total torque of the motor composed of the two contributions from each cylinder is calculated as

$$M_{tot} = M_{16} + M_{32} \quad (32)$$

The evolution of the total torque is given in Fig. 22.
The torque represented in Fig. 22 shows not identic contributions in the first and second half periods. This is due to the specific evolution of the pistons and their related speed in the two half periods. This corresponds to a system where the pistons are 180° phase shifted and where the same sides of the cylinders (left and right) are cascaded for the expansion.

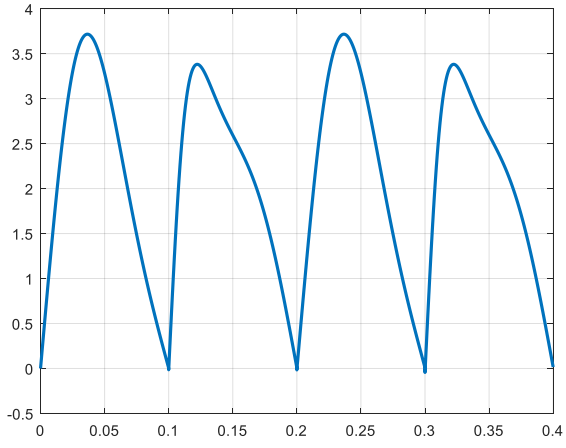

Fig. 22: Evolution of the total torque.

System with pistons in phase and cross connected expansion ways

For the mechanical coupling of the two cylinders, another possibility exists in changing the position of the pins on the crankshaft for a synchronous evolution of both pistons (same phase position). To obtain a similar expansion of the air, cross connected exchange lines between the cylinders must be chosen for the transfer of the air. This solution is called the zero angle shifted pistons. The corresponding diagram is shown in Fig. 23.

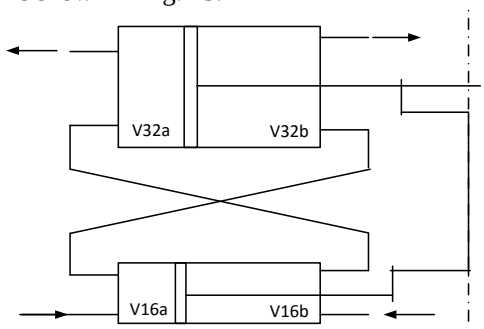

Fig. 23: System with pistons in phase and cross connected expansion ways.

For the system with pistons in phase and cross connection of the expansion ways, the two torque contributions are calculated (16 mm and 32 mm pistons).

Contributions of the small cylinder

The torque contribution of the small cylinder (16 mm cylinder) is represented in Fig. 24, and the torque contribution of the 32 mm cylinder is represented in Fig. 25.

The curve in Fig. 24 shows an evolution of the torque that is of similar amplitude in the first and second half periods. The marked difference in the maximum amplitudes that was typical of the system with 180° shifted pistons (see Fig. 17) is strongly reduced.

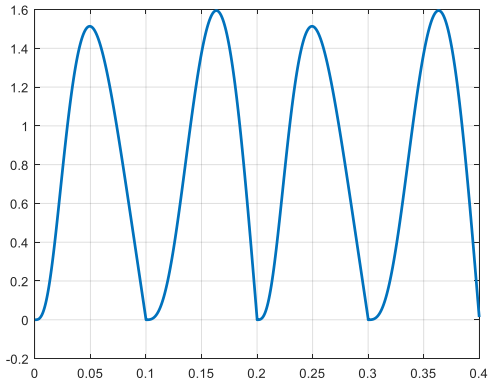

Fig. 24: Torque contribution of the 16 mm piston (in phase pistons and cross connection).

Contributions of the larger cylinder

The torque contribution of the larger cylinder (the 32 mm cylinder) is represented in Fig. 25. This time, the difference in the amplitudes of the maximum torque in the first and second period are marked.

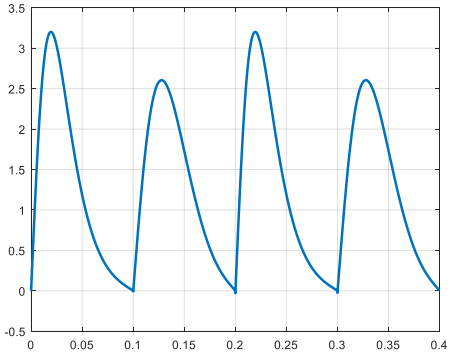

Fig. 25: Torque contribution of the 32 mm piston (in phase pistons and cross connection).

Total torque of the motor

The total torque developed by the motor with synchronous pistons is represented in Fig. 26 The curve shows less modulation as in the case of the motor with reciprocating pistons.

To show the difference between both systems, the two curves are superposed in Fig. 27.

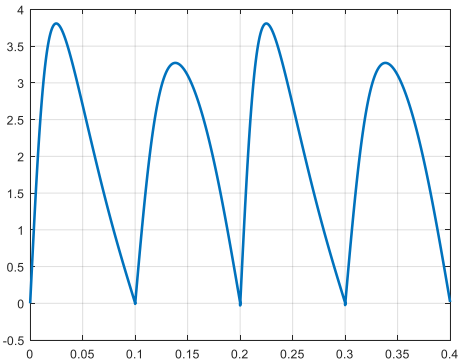

Fig. 26: Total torque of the system with zero phase shift of the pistons

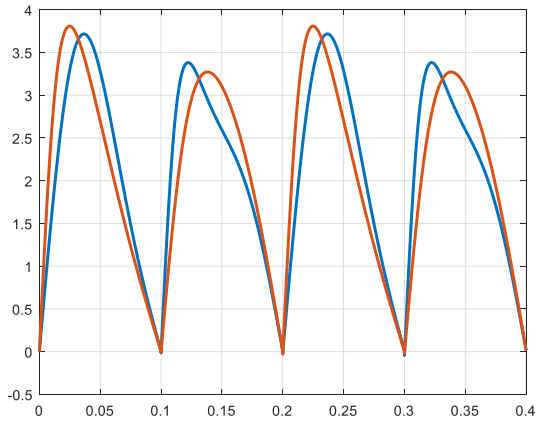

Fig. 27: Comparison of the total torques of the two systems (0° and 180° shifted pistons)

Energy converted and calculation of the efficiency.

Converted energy

The mechanical energy at the output of the pneumatic motor is calculated by integration of the power as was already done for the single cylinder. The curve showing the converted energy during the complete cycle (2 periods) is shown in Fig. 28.

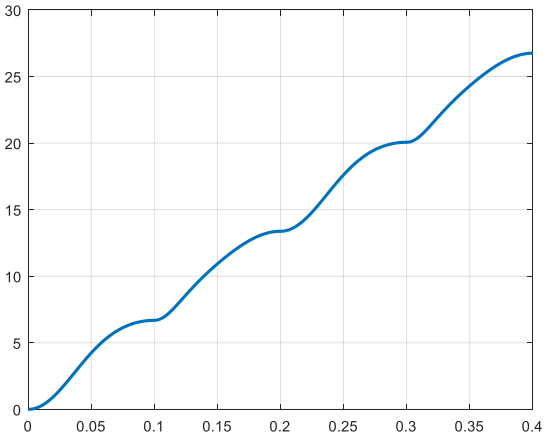

Fig. 28: Converted energy.

The energy amounts converted by the two systems as described in Fig. 10 and in Fig. 23 are represented in superposition in Fig. 29. The final values of the converted energy over the two periods are identic and reach the final value of 26.75 J

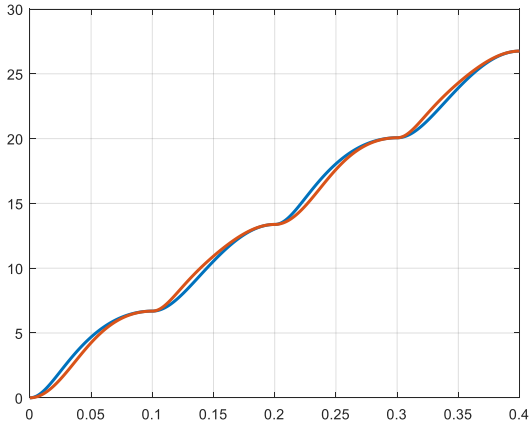

Fig. 29: Superposed curves of the converted energy by the two systems (0° and 180° shifted pistons

Efficiency of the system with expansion

The efficiency of the system with expansion is calculated on the base of the produced mechanical work and the injected enthalpy into the system. In fact, this enthalpy is identic to the enthalpy injected in the cylinder of the first motor (one cylinder only, rel. (20)

$$\eta_{conv} = \frac{W_{out}}{H_{in}} = \frac{W_{out}}{U+P_{in}\cdot\Delta V} \qquad (33)$$

The transmitted mechanical energy W_{out} is equal to 26.75 J as was described in the previous section

U is the thermodynamic content of the injected air under pressure and is calculated as the energy needed for the compression into V_1 of the equivalent mass of air from the atmospheric pressure to the value of P_{in}, V_1 being the filled volume of the first actuator during the total running period (0° to 4π).

$$U = E_{comp} = P_{in} \cdot V_1 \left(ln \frac{P_{in}}{P_{atm}} - 1 + \frac{P_{atm}}{P_{in}} \right) \quad (34)$$

Numerically, and considering the two complete cycles (ϕ =0…4π), U becomes

$$U = E_{comp} = 10 \cdot 10^5 N/m^2 \cdot 4 \cdot 4.02 \cdot 10^{-6} m^3 \cdot \left(ln \frac{10bar}{1bar} - 1 + \frac{1bar}{10bar} \right) = 22.5J \qquad (35)$$

$$P_{in} \cdot \Delta V = 10 \cdot 10^5 N/m^2 \cdot 4 \cdot 4.02 \cdot 10^{-6} m^3 = 16J \quad (36)$$

The efficiency becomes

$$\eta_{conv} = \frac{W_{out}}{H_{in}} = \frac{26.75J}{16J+22.55J} = 0.693 \qquad (37)$$

Comparison of the mechanical work

The mechanical work obtained at the output of the two systems, namely the single cylinder motor and the motor with cascaded cylinders with expansion are represented in Fig. 30 for comparison. The figure shows that the energy converted by adding an expansion chamber can be nearly doubled. This is fully compatible with the energy efficiencies calculated for the two systems (rel. 18 and rel. 33).

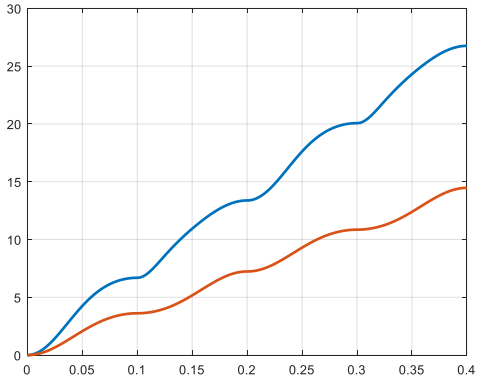

Fig. 30: Comparison of the produced works.

Experimental set-up

An experimental set-up of a system with 180° shifted crankshaft pins has been realized. The pneumatic cylinders are of 16 mm diameter, respectively 32 mm. The stroke is equal to 20 mm. The system is controlled from a position sensor mounted on the rotating shaft. The air valves are controlled according the sequential diagram of Fig. 31. The whole system with its control electronics is represented schematically in Fig.32.

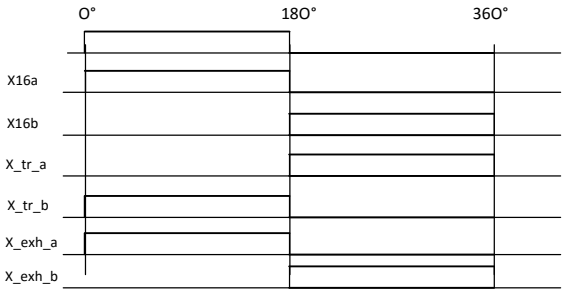

Fig. 31: Control sequence of the pneumatic valves

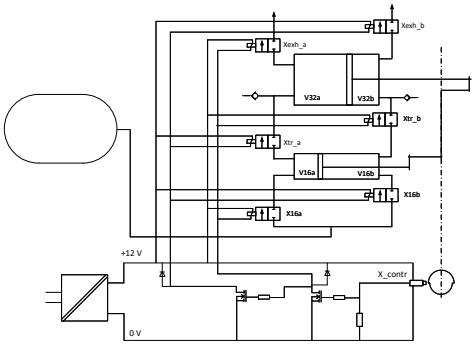

Fig. 32: Pneumatic motor assembly with control of the pneumatic valves.

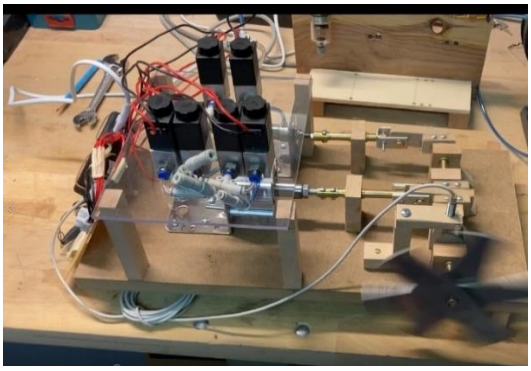

Fig. 33: Experimental set-up with two cylinders

Displacement work and expansion in the same cylinder

Basic principle

The principle described previously has the interesting property to strongly increase the energetic efficiency. The principle is based on the association of a displacement work realized in a first cylinder, and of an additional expansion work in a second one. The possibility however exists to combine the two contributions of mechanical work in one cylinder only. For such a system, one cylinder of the size of the second cylinder of the previous two-cylinder system is chosen, leading to an identical final volume of the expansion. The intake of air is chosen identical to the volume of the small cylinder of the previous system but is realized inside of the same cylinder as for the expansion. The intake corresponding to the displacement work is so realized during a partial stroke of the single cylinder, and the expansion is realized during the remaining part of the same stroke. Consequently, the control of the intake and exhaust valves must be newly defined.

Additionally, the evolution of the volumes of the left- and-right-side chambers of the cylinder being asymmetric, the intake angles of the crankshaft will also be different for the two chambers.

The principle of realizing the displacement work and the expansion work in the same cylinder has been already proposed for a classical engine [11] and is adapted in this study for a motor based on a double effect linear cylinder as used in the previous paragraphs.

Asymmetrical evolution of the piston and design of the intake angles

An interesting property of the motor is given by the asymmetric evolution of the piston in its descending and ascending motions. The asymmetric evolution can be observed on the curve of the piston's velocity as shown in Fig. 34.

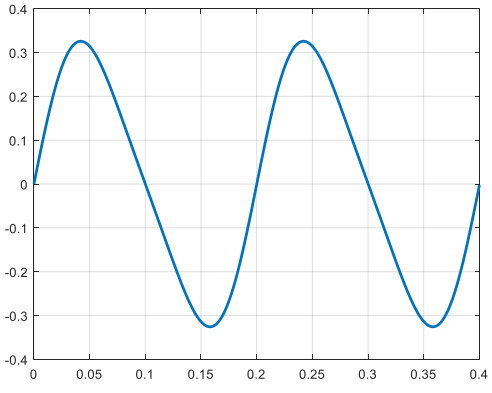

Fig. 34: Evolution of the speed of the piston in the linear cylinder.

Especially, the rise of the speed in the first quarter of period is faster than the rise in the third quarter.

The study of the system given in this section is based on a cylinder having the same parameters as the larger one of the double cylinder system of the previous sections. The displacement work is also adjusted to the value as in the previous system, with a corresponding volume being equal to one fourth of the volume of the larger cylinder. As a result, the displacement work as well as the expansion work of the motor with displacement/expansion in the same cylinder will be theoretically identical to the values of the two-cylinder motor.

The consumption of air from the pressurized reservoir is also identical to the consumption of the double cylinder system.

The displacement work of the descending stroke is defined, in addition to the value of the pressure and the piston's surface, through the length of the displacement as indicated with the parameter x_{int_a} in Fig. 35. For a cylinder having a maximal stroke of 20mm, the displacement length must be chosen as 5mm (1/4 of the maximal stroke).

The displacement work of the ascending stroke is defined through the length of the displacement as indicated with the parameter x_{int_b} in Fig. 35. This parameter is chosen as identic to the displacement length x_{int_a} of the descending stroke.

$$x_{int\_b} = x_{int\_a} = \frac{1}{4} \cdot 20mm = 0.005m \qquad (38)$$

Fig. 34 defines the parameter x_{int_b0} for the ascending stroke

$$x_{int\_b0} = x_{stroke\_max} - x_{int\_b} = 0.020\text{m} - 0.005\text{m} = 0.015\text{m}$$

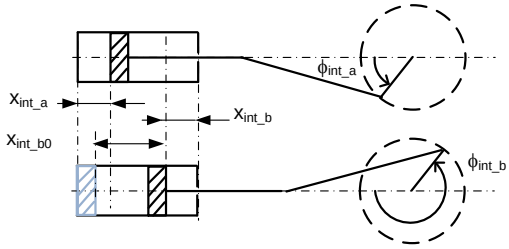

Fig. 35: Lengths of the displacements in descending and ascending motions.

From rel. (1), the lengths of the displacements are defined as

$$x_{int\_a} = r(1 - cos\,\varphi_{int\_a}) + \frac{\lambda}{2} r\,sin^2\,\varphi_{int\_a} \qquad (39)$$

$$x_{int\_b0} = r(1 - cos\,\varphi_{int\_b0}) + \frac{\lambda}{2} r\,sin^2\,\varphi_{int\_b0} \qquad (40)$$

The values of the rotation angles of the crankshaft f_{int_a} and f_{int_b0} to move the piston up to the positions of x_{int_a} and x_{int_b0} are obtained through successive approximations using the relations (39) and (40), namely

$$\varphi_{int\_a} = 53.5° \qquad (41)$$

$$\varphi_{int\_b\,0} = 247.5° \qquad (42)$$

These angles correspond to the position of the crankshaft where the intake valves have to be closed, respectively where the expansion work begins in the chambers.

To design the real intake angles for the descending and ascending strokes, the following angles for the openings of the intake valves are given

$$\varphi_{int\_a\_open} = 0° \qquad (43)$$

$$\varphi_{int\_b\_open} = 180° \qquad (44)$$

The real intake angles become

$$\varphi_{int\_a} = 53.5° \qquad (45)$$

$$\varphi\ int\_b\ 0_{int\_b} \qquad (46)$$

The difference between these two values is in relation with

the asymmetrical motion in the descending and ascending strokes as described at the beginning of this section.
For the exhaust of the expanded air, the openings and closings of the exhaust valves are

$\varphi_{exh\_a\_open} = 180°$ (47)

$\varphi_{exh\_a\_close}$ (48)

$\varphi_{exh\_b\_open} = 0°(or 360°)$ (49)

$\varphi_{exh\_b\_close}$ (50)

Control of the valves

From the definitions of the previous paragraph, the control sequences of the intake and exhaust valves can be defined. The evolution of the signals is represented in Fig. 36. The signal names are explicit.

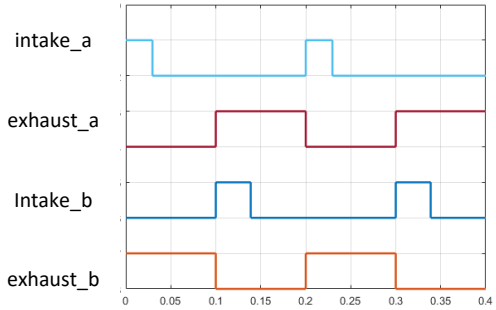

Fig. 36: Control signals for the intake and exhaust valves.

From the sequence diagram of Fig. 36, three independent position sensors are needed. The first is controlling the intake valve at side a of the piston:

Intake_a = Xin_a (51)

The second sensor controls directly the intake valve at the b side of the piston

Intake_b = xin_b (52)

For the two exhaust valves, only one sensor is needed. Its signal (zeropi) changes all 180°.
The control signals are generated according

$exhaust\_a = \overline{zeropi}$ (53)

$exhaust\_b = zeropi$ (54)

Figure 37 shows the elements of the sensor system. The sensors can be for example of the ferrostatic type, reacting to the presence of a ferromagnetic surface (black sectors on the rotating disks).

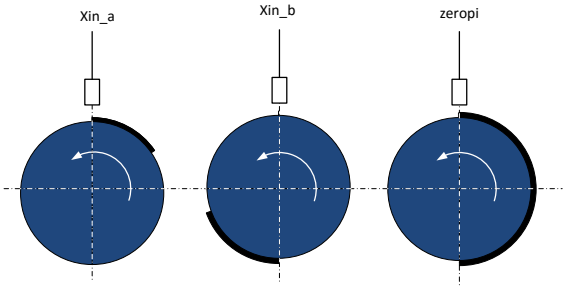

Fig. 37: Position sensors for the control of the intake and exhaust valves.

A global schematic diagram of the system with its control and position sensors is given in Fig. 38.

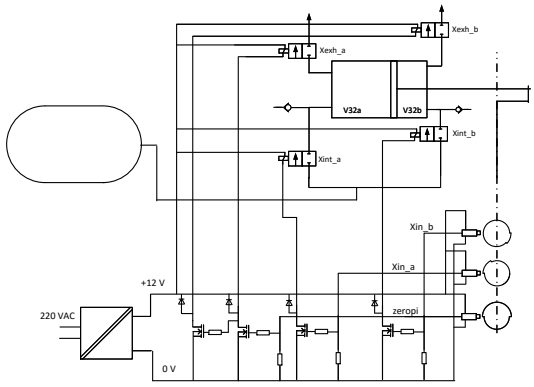

Fig. 38: Schematic diagram of the system with control and sensors.

Evolution of the volumes of the chambers

The evolution of the volumes of each chamber (a and b side of the piston) are represented in Fig. 39 and 40. The curves show the same asymmetry of the rate of change of both volumes.

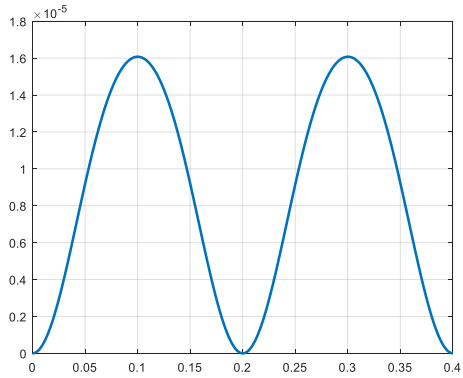

Fig. 39: Evolution of the volume of chamber a

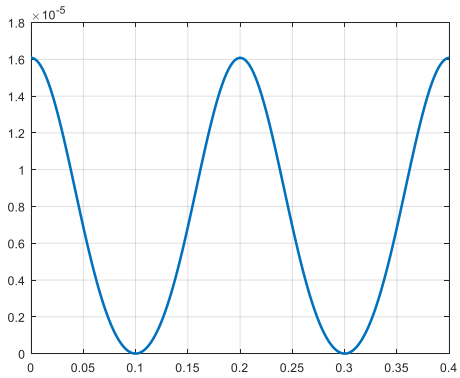

Fig. 40: Evolution of the volume of chamber b

Force exerted on the piston

The force exerted on the piston is given by the pressure multiplied by the piston's surface. In Fig. 41, the total force is represented as the sum of different components:

- Force on the a-side of the piston given by the pressure during intake and expansion
- Force on the b-side of the piston given by the pressure during intake and expansion
- Forces on the a and b-sides of the piston given by the atmospheric pressure during exhaust

The force is positive during the first half-period (motion from left to the right), and is negative during the second half-period (motion from the right to the left). It is easy to

understand the constant value of the force during the intake, when the pressure is constant, and the typical decrease during expansion.

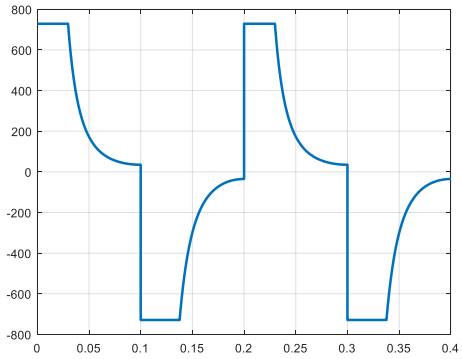

Fig. 41: Total force exerted on the piston.

Torque and power

With the goal to evaluate the waveform of the torque, the same method as in the previous sections is used, namely the indirect calculation through the instantaneous value of power. This value is the product of the force multiplied by the piston's velocity and is represented in Fig. 42. This representation shows different values of the maxima of the power during the descending and ascending strokes. This difference is caused by the different velocities of the piston, even if the value of the force is the same during both intakes.

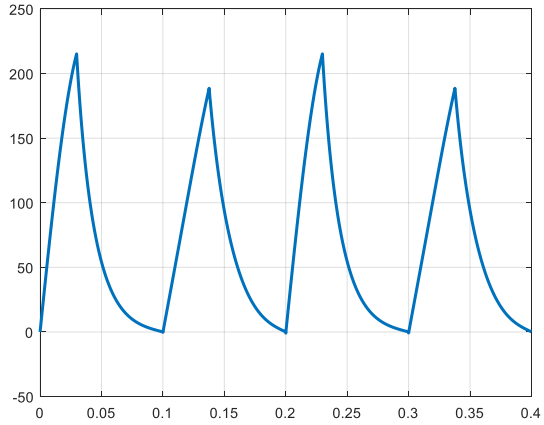

Fig. 42: Mechanical power transmitted to the crankshaft

The value of the torque is then obtained by dividing the power by the angular velocity of the crankshaft. The corresponding curve is given in Fig. 43.

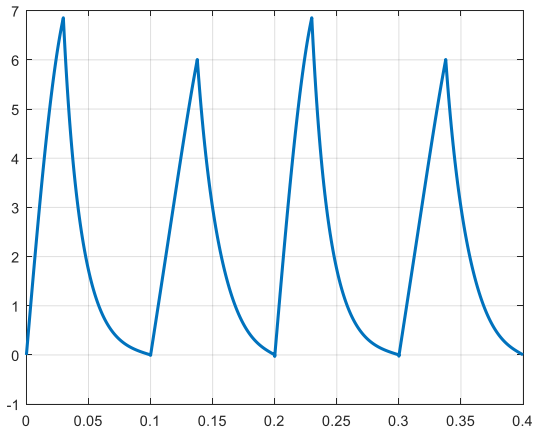

Fig. 43: Torque produced by the motor.

Mechanical work produced

The mechanical work produced is obtained by integration of the power over the two periods. The corresponding curve is given in Fig. 44. The final value of the produced work is 26.85 J. This value corresponds to the work produced by the system using two cylinders described through Fig. 28.

A small difference is observed (26.75J instead of 26.85J) but is due to the precision of the simulation. The two systems must theoretically produce the same amount of work, because they are characterized both by a displacement at constant pressure over the same volume, followed by an expansion of the same amount of air with an identic volume ratio.

The pointed shape of the torque of the system with one cylinder (Fig. 43) can be the reason of the small difference obtained in the simulation.

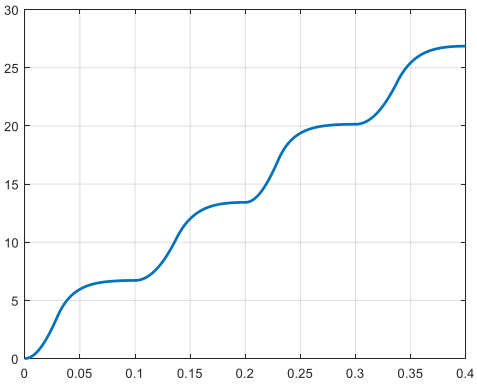

Fig. 44: Mechanical work produced by the system with displacement and expansion in the same cylinder.

Conclusions

A high efficiency pneumatic motor based on double-acting linear cylinders is proposed, which consists in a tandem operation of a small cylinder and a larger-one coupled to a common crankshaft. The energetic performance of this motor is nearly doubled in comparison to a classical system using only one cylinder and operating with displacement work under constant pressure and having the same air consumption.

A simplified version using only one cylinder for the association of displacement and expansion work is also proposed and have similar energetic performance. This new system needs however a more complex position sensor and control circuit for the intake and exhaust valves.

References

1. Hussein Ibrahima, Karim Belmokhtara, Mazen Ghandourb, Investigation of Usage of Compressed Air Energy Storage for Power Generation System Improving - Application in a Microgrid Integrating Wind Energy, 9th International Renewable Energy Storage Conference, IRES 2015, Energy Procedia 73 (2015) 305 – 316
2. Laijun CHEN1, Tianwen ZHENG1, Shengwei MEI1, Xiaodai XUE1, Binhui LIU1, Qiang LU1 Review and prospect of compressed air energy storage system, J. Mod. Power Syst. Clean Energy (2016) 4(4):529–541DOI 10.1007/s40565-016-0240-5
3. Rufer A., Energy storage – Systems and components, CRC Press
4. S. Lemofouet-Gatsi, Investigation and optimisation of hybrid electricity storage systems based on compressed air and supercapacitors, PhD Thesis, EPFL, École

Polytechnique Fédérale de Lausanne, 2006, DOI 10.5075/epfl-thesis-3628
5. Heidari, Mahbod, Contribution to the Technique of Compressed Air Energy Storage The Concept of Finned Piston PhD Thesis, EPFL, École Polytechnique Fédérale de Lausanne, 2015, DOI 10.5075/epfl-thesis-6738
6. Luis Carlos Mendoza, Sylvain Lemofouet , Jürg Schiffmann, Testing and modelling of a novel oil-free co-rotating scroll machine with water injection, Applied Energy 185 (2017) 201–213
7. Garvey S., et al: Compressed air energy storage has bags of potential. University of Nottingham, 2012. https://www.theengineer.co.uk/issues/25-april-2011/compressed-air-energy-storage-has-bags-of-potential/
8. Maxim de Jong, Commercial Grid Scaling of Energy bags for Underwater Compressed Air Energy storage, Proceedings of the 2014 Offshore Energy & Storage Symposium, Windsor, Ontario. Canada, UWCAES Society, July, 10-11, 2014 http://www.tandfonline.com/doi/full/10.1080/00207233.2014.947726?scroll=top&needAccess=true
9. Richard J., Noca F., Stockage sous-marin d'énergie, Bulletin Electrosuisse, 3/2017, https://www.strom.ch/fr/services/bulletin
10. Rufer A. A Compressed Air Driven Generator with Enhanced Energetic Efficiency, Conference IEMERA 2020, Imperial College, London October 2020.
11. Vito Gianfranco Truglia, High-Efficiency Engine Driven by Pressurized Air or Other Compressible Gases, Patent No US 9.677.400 B2, Jun. 13, 2017.